Advances in Applied Mathematics and Mechanics
Adv. Appl. Math. Mech., Vol. **1**, No. 3, pp. 438-450 (2009)

June 2009

LWDG Method for a Multi-Class Traffic Flow Model on an Inhomogeneous Highway

Tiantian Sun[1] and Jianxian Qiu[1,*]

[1] *Department of Mathematics, Nanjing University, Nanjing, Jiangsu 210093, China*

Received 12 February 2009; Accepted (in revised version) 01 April 2009
Available online 22 April 2009

Abstract. In this paper, we apply the discontinuous Galerkin method with Lax-Wendroff type time discretizations (LWDG) using the weighted essentially non-oscillatory (WENO) limiter to solve a multi-class traffic flow model for an inhomogeneous highway. This model is a kind of hyperbolic conservation law with spatially varying fluxes. The numerical scheme is based on a modified equivalent system which is written as a "standard" hyperbolic conservation form. Numerical experiments for both the Riemann problem and the traffic signal control problem are presented to show the effectiveness of the method.

AMS subject classifications: 35L65, 65M60

Key words: Multi-class traffic flow; inhomogeneous highway; spatially varying flux; non-strictly hyperbolic conservation laws; LWDG method; WENO limiter.

1 Introduction

The first discontinuous Galerkin (DG) method was introduced in 1973 by Reed and Hill [18], in the framework of neutron transport (steady state linear hyperbolic equations). A major development of the DG method was carried out by Cockburn et al. in a series of papers [2–6], in which a framework was established to solve *nonlinear* hyperbolic conservation laws:

$$\begin{cases} u_t + \nabla \cdot f(u) = 0, \\ u(x,0) = u_0(x). \end{cases} \tag{1.1}$$

They proposed to use an explicit, nonlinear stable and high order Runge-Kutta time discretizations [19] and DG discretization in space with exact or approximate Riemann solvers as interface flux and limiters such as the total variation bounded (TVB) limiters [20] or weighted essential non-oscillatory (WENO) type limiters [15, 16] to

*Corresponding author.
URL: http://math.nju.edu.cn/∼jxqiu/index.htm
Email: asmaphy84@yahoo.com.cn (T. Sun), jxqiu@nju.edu.cn (J. Qiu)

achieve nonoscillatory properties for strong shocks. The method is termed as Runge-Kutta discontinuous Galerkin method (RKDG). The DG method has following advantages: Easy handling of complicated geometry and boundary conditions (common to all finite element methods), allowing hanging nodes in the mesh; Compact, communication only with immediate neighbors, regardless of the order of the scheme; Explicit, because of the discontinuous basis, the mass matrix is local to the cell, resulting in explicit time stepping (no systems to solve); Parallel efficiency, achieves 99% parallel efficiency for static mesh and over 80% parallel efficiency for dynamic load balancing with adaptive meshes [1].

An alternative approach to discretize the time derivative term could be using a Lax-Wendroff type time discretization procedure, which is also called the Taylor type referring to a Taylor expansion in time. This approach is based on the idea of the classical Lax-Wendroff scheme [11], and it relies on converting all the time derivatives in a temporal Taylor expansion into spatial derivatives by repeatedly using the PDE and its differentiated versions. The spatial derivatives are then discretized by the DG approximations. The Lax-Wendroff type time discretization, which is also referred to as the Taylor-Galerkin method for the finite element methods, usually produces the same high order accuracy with a smaller effective stencil than that of the Runge-Kutta time discretization, and it uses more extensively the original PDE. Since the Lax-Wendroff time discretization is an one step method instead of the multi-step Runge-Kutta time discretization, the LWDG method can save a certain amount of computational cost over the RKDG method, thus is more cost effective.

Lighthill and Whitham [13] and Richards [17] independently proposed a simple continuum model, known as the LWR model, to describe the characteristics of traffic flow. In this model, a traffic stream model (relationship between traffic state variables of flow, speed and density, e.g., [10]) is supplemented by the continuity equation of vehicles, and the resulting partial differential equation presumably could be solved to obtain the density as a function of space and time. Although aiming at providing a coarse representation of traffic behavior, the LWR model is capable of reproducing qualitatively a remarkable amount of real traffic phenomena such as shock formation. However, there are still some puzzling traffic phenomena that this simple LWR model cannot address or explain, such as the two-capacity or reverse-λ state in the fundamental diagram, hysteresis of traffic flow and platoon dispersion.

Recently, multi-class models (MCLWR models) have been developed in an attempt to explain these puzzling traffic phenomena by modeling users' lane changing behavior and multiple vehicle types [7, 8]. Although the MCLWR model is simple in nature, it was found that the model is capable of producing the desired properties of a macroscopic traffic flow model and it explains many puzzling phenomena mentioned before. In [23], the MCLWR model was solved by a first-order Lax-Friedrichs finite difference scheme. However, this scheme may produce smeared solutions near discontinuities due to excessive numerical viscosity. Then Lebacque [12] successfully applied the Godunov scheme, introduced by Godunov [9], to solve the LWR model. It is subject to smaller numerical viscosity, but requires a Riemann solver as its building block,

which is very difficult even impossible to develop for the MCLWR model. In [25], a high-order WENO scheme is applied to solve the MCLWR model. This scheme is more efficient than the low-order Lax-Friedrichs and Godunov schemes.

In this paper, we apply the LWDG method using WENO limiter to solve the MCLWR model on an inhomogeneous highway. Firstly, we define all the necessary variables in this model:

- The number of lanes: $a(x)$;
- The free flow(maximum) velocities of m types of vehicles: $\{v_{l,f}(x)\}_{l=1}^{m}$;
- The density per lane of the lth type: $\rho_l(x,t)$;
- The total density per lane: $\rho(x,t)=\sum_{l=1}^{m}\rho_l(x,t)$;
- The velocity of the lth type of vehicles: $v_l(\rho)$;
- The maximum of the free flow velocities $v_{l,f}(x)$ of the lth type at location x: $v_f \equiv \max_x \max_{1\le l\le m}(v_{l,f}(x))$.

Furthermore, we assume that $\{v_l\}_{l=1}^{m}$ are related by

$$v_l = b_l(x)v(\rho), \quad v'(\rho)<0, \quad b_l(x)=v_{l,f}(x)/v_f. \tag{1.2}$$

Accordingly, $\{b_l(x)\}_{l=1}^{m}$ represent the velocity differences between m vehicles and $0\le b_l(x)\le 1$.

Then we derive the model equations from the mass conservation of m types of vehicles, which read

$$(a(x)\rho_l)_t + (a(x)\rho_l b_l(x)v(\rho))_x = 0, \quad 1\le l\le m. \tag{1.3}$$

Eq. (1.3) is a natural extension of the MCLWR model. For convenience, we introduce the conservative solution variables $u_l=a(x)\rho_l$, and the component of flux $f_l=b_l u_l v(\sum u_l/a)$. Thus we get the solution vector $u=(u_1,\dots,u_m)^T$ and the flux vector $f=(f_1,\dots,f_m)^T$. Accordingly, the model equations can be written as

$$u_t + f_x(u,\theta(x)) = 0, \tag{1.4}$$

where $\theta(x)$ represents all inhomogeneous factors on the road, namely,

$$\theta(x) = \Big(a(x), b_1(x), \dots, b_m(x)\Big).$$

In this traffic flow problem, each density ρ_l and the total density ρ are bounded by a jam density ρ_{jam}, and thus

$$u/a\in\overline{D}, \quad \overline{D}=\Big\{u/a|\rho_l\ge 0, l=1,\dots,m; \sum_{l=1}^{m}\rho_l\le\rho_{jam}\Big\}. \tag{1.5}$$

Moreover, the function $v(\rho)$ of (1.2) satisfies

$$v(0)=v_f, \quad v(\rho_{jam})=0.$$

This traffic system has significant practical meaning in real world. For instance, the changes of value of $\theta(x)$ represents the drop or increase in traffic capacity at corresponding locations, such as road junctions, curves and slopes and traffic accidents. In particular, $b_l=b_l(x,t)$ can serve as a switch function in traffic signal problem, as is shown in Section 3. These changes are usually very sharp, so all the coefficients in θ can be treated as being discontinuous at the change. This means the flux $f(u,\theta(x))$ is a discontinuous function of location x through the discontinuous function $\theta(x)$. As is pointed out in [26], it is usually impossible (for $m>2$) to solve the eigen-polynomial of system (1.4) explicitly, let alone the solutions to Riemann problems. Thus we can only use approximate Riemann solvers such as the Lax-Friedrichs solvers for numerical schemes. It will be not be efficient to apply the numerical schemes for conservation laws, such as TVD, WENO and RKDG, to solve the traffic system with discontinuous flux. In order to overcome this problem, we need to transform system (1.4) into "standard" conservation form, and all our following discussions are under the modified equivalent system of (1.4), in which all of the components of θ are variables. In this case, the hyperbolicity of the system can be proved, and the wave patterns of the Riemann problem can also be predicted [26].

In this paper, the LWDG method is applied to the modified system. The organization of this paper is as follows. In section 2, we describe in detail the construction and implementation of the LWDG method for a multi-class traffic flow model. In section 3 we provide numerical examples to demonstrate the behavior of the schemes. Concluding remarks are given in section 4.

2 Description of LWDG for a multi-class traffic flow model

A Lax-Wendroff type time discretization procedure for the discontinuous Galerkin method has been developed to solve hyperbolic conservation laws in [14]. Now we apply this method to this traffic flow model of one-dimensional system conservation laws.

For convenience, we treat θ as a scalar in the following discussions, but the results are applicable to the system case. Consider the modified equivalent system

$$U_t + F(U)_x = 0, \tag{2.1}$$

where

$$U(x,t) = \Big(u^1(x,t),\dots,u^{m+1}(x,t)\Big)^T = \Big(a(x)\rho_1(x,t),\dots,a(x)\rho_m(x,t),a(x)\Big)^T,$$

is a vector and

$$F(U) = \Big(f^1(u^1,\dots,u^{m+1}),\dots,f^{m+1}(u^1,\dots,u^{m+1}\Big)^T,$$

is a vector function of U.

We denote the cells by $I_i=[x_{i-\frac{1}{2}}, x_{i+\frac{1}{2}}]$, the cell centers by $x_i=\frac{1}{2}(x_{i-\frac{1}{2}}+x_{i-\frac{1}{2}})$, and the cell sizes by $\Delta x_i=x_{i+\frac{1}{2}}-x_{i-\frac{1}{2}}$. Let Δt be the time step, $t^{n+1}=t^n+\Delta t$. By the temporal Taylor expansion we obtain

$$U(x,t+\Delta t)=U(x,t)+\Delta t U_t+\frac{\Delta t^2}{2}U_{tt}+\frac{\Delta t^3}{6}U_{ttt}+\dots. \tag{2.2}$$

If we would like to obtain $(k+1)$th order accuracy in time, we would need to approximate the first $k+1$ time derivatives. In this paper we will proceed up to third order in time and the procedure can be naturally extended to any higher orders.

The temporal derivative terms in (2.2) can be replaced with the spatial ones component by component using the original equations (2.1):

$$U_t=-F(U)_x=-F^{'}(U)U_x, \tag{2.3}$$
$$U_{tt}=-(F^{'}(U)U_x)_t=-(F^{'}(U)U_t)_x=-F^{'}(U)_xU_t-F^{'}(U)U_{xt}, \tag{2.4}$$
$$U_{xt}=-F^{'}(U)_xU_x-F^{'}(U)U_{xx}, \tag{2.5}$$
$$U_{ttt}=-(F^{'}(U)_tU_t+F^{'}(U)U_{tt})_x, \tag{2.6}$$

where U_x, U_t, U_{xt}, U_{xx}, U_{tt} are vectors whose component is the corresponding derivative of each component of U, $F^{'}(U)$ is the Jacobian matrix of (2.1), and $F^{'}(U)_x, F^{'}(U)_t$ can be viewed as the matrix whose components are the corresponding derivative of each component of $F^{'}(U)$.

Then we can write the approximation to (2.2) up to third order as:

$$U(x,t+\Delta t)=U(x,t)-\Delta t\widetilde{F}_x, \tag{2.7}$$

with

$$\widetilde{F}=F+\frac{\Delta t}{2}(F^{'}(U)U_t)+\frac{\Delta t^2}{6}(F^{'}(U)_tU_t+F^{'}(U)U_{tt}).$$

The standard discontinuous Galerkin method is then used component by component to discretize $\widetilde{F}_x$ in (2.7), as described in detail below.

The test function space is given by $V_h^k=\{p: p|_{I_i}\in P^k(I_i)\}$, where $P^k(I_i)$ is the space of polynomials of degree $\le k$ on the cell I_i. We adopt a local orthogonal basis over I_i, $\{v_l^{(i)}(x), l=0,1,\dots,k\}$, namely the Legendre polynomials

$$v_0^{(i)}(x)=1,\quad v_1^{(i)}(x)=\frac{x-x_i}{\Delta x_i},\quad v_2^{(i)}(x)=(\frac{x-x_i}{\Delta x_i})^2-\frac{1}{12},\dots.$$

Other basis functions can be used as well, without changing the numerical method, since the finite element discontinuous Galerkin method depends only on the choice of space V_h^k, not on the choice of its basis functions.

The numerical solution $U^h(x,t)$ in the space V_h^k can be written as:

$$U^h(x,t)=\sum_{l=0}^{k}U_i^{(l)}(t)v_l^{(i)}(x),\quad \text{for}\quad x\in I_i,$$

and the degrees of freedom $U_i^{(l)}(t)$ are the moments defined by

$$U_i^{(l)}(t) = \frac{1}{a_l}\int_{I_i} U^h(x,t)v_l^{(i)}(x)dx,\ l = 0,1,\ldots,k,$$

where $a_l = \int_{I_i}(v_l^{(i)}(x))^2dx$ are the normalization constants since the basis is not orthonormal. In order to determine the approximate solution, we evolve the degrees of freedom $U_i^{(l)}$:

$$U_i^{(l)}(t^{n+1}) = U_i^{(l)}(t^n) - \frac{\Delta t}{a_l}\Big(-\int_{Ii}\widetilde{F}\frac{d}{dx}v_l^{(i)}(x)dx + \hat{\widetilde{F}}_{i+\frac{1}{2}}v_l^{(i)}(x_{i+\frac{1}{2}}) - \hat{\widetilde{F}}_{i-\frac{1}{2}}v_l^{(i)}(x_{i-\frac{1}{2}})\Big),\quad l = 0,1,\ldots,k, \tag{2.8}$$

where $\hat{\widetilde{F}}_{i+\frac{1}{2}}$ is a numerical flux which depends on the values of numerical solution u^h and its spatial derivatives at the cell interface $x_{i+\frac{1}{2}}$, both from the left and from the right. This numerical flux is related to the so-called generalized Riemann solvers [22]. As indicated before, for $m>2$, it is impossible to achieve the solutions to the Riemann problems. Thus in this paper, we use the following simple Lax-Friedrichs flux

$$\hat{\widetilde{F}}_{i+\frac{1}{2}} = \frac{1}{2}\Big(\widetilde{F}^-_{i+\frac{1}{2}} + \widetilde{F}^+_{i+\frac{1}{2}} - \alpha(U^+_{i+\frac{1}{2}} - U^-_{i+\frac{1}{2}})\Big).$$

Here $U^{\pm}_{i+\frac{1}{2}}$ and $\widetilde{F}^{\pm}_{i+\frac{1}{2}}$ are the left and right limits of the discontinuous solution U^h and the flux $\widetilde{F}$ at the cell interface $x_{i+\frac{1}{2}}$, and

$$\alpha = \max_U \rho(F^{'}(U)). \tag{2.9}$$

where $\rho(F^{'}(U))$ is the spectral radius of the Jacobian matrix $F^{'}(U)$. The integral term in (2.8) can be computed either exactly or by a suitable numerical quadrature accurate to at least $\mathcal{O}(\Delta x^{k+l+2})$. In this paper we used four points Gauss-Lobatto quadratures for $k = 2$.

As indicated in [15], if the solutions have strong discontinuities, the original LWDG scheme will generate significant oscillations and even nonlinear instability. In this paper we adopt the WENO limiter developed in [15] for LWDG method. The idea is to first identify "troubled cells", namely those cells where limiting might be needed, then to abandon all moments in those cells except the cell averages and reconstruct those moments from the information of neighbouring cells using a WENO methodology. Unlike the RKDG methods, by which the limiting procedure is performed in every inner Runge-Kutta stage, we only need to perform the limiting procedure once per time step for the one step LWDG method. For the case of system, the DG discretization is performed on each component. And in order to achieve better qualities at the price of more complicated and costly computations, we use a local characteristic decomposition in the limiting procedure. For the details of such local characteristic field decompositions, we refer to [21]. The limiter and the WENO reconstructions are all performed under local characteristic projections.

3 Numerical results

In this section, we show the numerical results for both the Riemann problem and the traffic signal control problem by LWDG and RKDG methods described in Section 2. We will only show the test results for the third order LWDG and RKDG methods to save the space. In all the computation, we take CFL number CFL=0.12 for LWDG method, and CFL=0.18 for RKDG method. The TVB limiter with TVB constant M=10 is used as "troubled cell" indicator, and WENO reconstruction is applied to reconstruct the first and second moments in the troubled cell.

The velocities of (1.2) are set to be linear [10], $v(\rho) = v_f(1-\rho/\rho_{jam})$. In all of the illustrations, the densities ρ_l and ρ are scaled by ρ_{jam} so that we can assume $0 \le \rho_l, \rho \le 1$, and the spatial and temporal lengths L and T of the computational domain $(0,L)\times(0,T)$ are scaled to $(0,1)\times(0,T/L)$.

Example 3.1. We consider the Riemann problem with $b_l(x)(l=1,2,3)$ are constants,

$$b_1(x)=0.5, \quad b_2(x)=0.75, \quad b_3(x)=1, \quad L=8000m, \quad T=400s, \quad v_f=20m/s,$$

where T is the simulation time, and with following scaled initial conditions:

(a) $(a,\rho_1,\rho_2,\rho_3) = \begin{cases}(3,0.02,0.03,0.02), & \text{if } x \le 0.2,\\ (1,0.15,0.05,0.1), & \text{if } x > 0.2,\end{cases}$

(b) $(a,\rho_1,\rho_2,\rho_3) = \begin{cases}(3,0.1,0.05,0.05), & \text{if } x \le 0.5,\\ (2,0.2,0.1,0.3), & \text{if } x > 0.5,\end{cases}$

(c) $(a,\rho_1,\rho_2,\rho_3) = \begin{cases}(2,0.3,0.25,0.15), & \text{if } x \le 0.5,\\ (3,0.15,0.2,0.25), & \text{if } x > 0.5,\end{cases}$

(d) $(a,\rho_1,\rho_2,\rho_3) = \begin{cases}(2,0.4,0.1,0.2), & \text{if } x \le 0.35,\\ (3,0.3,0,0.1), & \text{if } x > 0.35.\end{cases}$

Under these assumptions, by Section 2, the Jacobian matrix $F'(U)$ in Eq. (2.3) can be written as:

$$F'(U) = \begin{pmatrix} a_{11} & -\frac{1}{u_4}v_f b_1 u_1 & -\frac{1}{u_4}v_f b_1 u_1 & \frac{1}{u_4^2}v_f b_1 u_1(u_1+u_2+u_3) \\ -\frac{1}{u_4}v_f b_2 u_2 & a_{22} & -\frac{1}{u_4}v_f b_2 u_2 & \frac{1}{u_4^2}v_f b_2 u_2(u_1+u_2+u_3) \\ -\frac{1}{u_4}v_f b_3 u_3 & -\frac{1}{u_4}v_f b_3 u_3 & a_{33} & \frac{1}{u_4^2}v_f b_3 u_3(u_1+u_2+u_3) \\ 0 & 0 & 0 & 0 \end{pmatrix},$$

where

$$a_{11} = v_f b_1\left(1-\frac{u_2+u_3}{u_4}\right) - \frac{2v_f b_1 u_1}{u_4},$$
$$a_{22} = v_f b_2\left(1-\frac{u_1+u_3}{u_4}\right) - \frac{2v_f b_2 u_2}{u_4},$$
$$a_{33} = v_f b_3\left(1-\frac{u_1+u_2}{u_4}\right) - \frac{2v_f b_3 u_3}{u_4}.$$

Then we can calculate the derivatives of each component of $F'(U)$ with respect to x and t to get $F'(U)_x$ in Eq. (2.4) and $F'(U)_t$ in Eq. (2.6).

In Table 1, we provide a CPU time comparison between LWDG and RKDG methods. The computation is performed on a Dell OptiPlex GX620nSF, P4-3.20 with 1GB ram. We can see

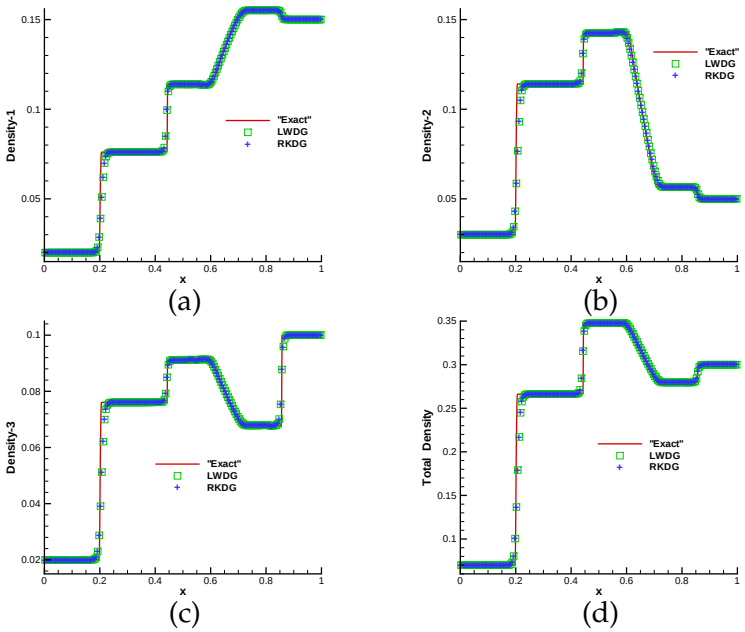

Figure 1: Example 3.1: The computed densities by the third order LWDG (Green Square) and the third order RKDG (Blue Plus) with $N = 200$ cells at $t = 0.05$, against the reference solutions (Red Solid Lines) by the third order RKDG with $N = 2000$ cells for initial condition (a); The ρ_1, ρ_2, ρ_3 and total density are plotted in subfigures (a)-(d), respectively.

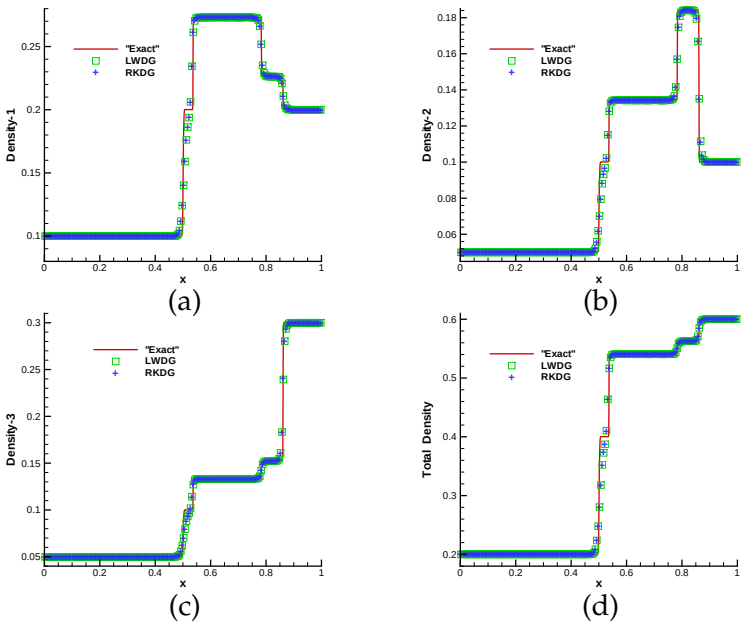

Figure 2: Same as Fig. 1, except for initial condition (b).

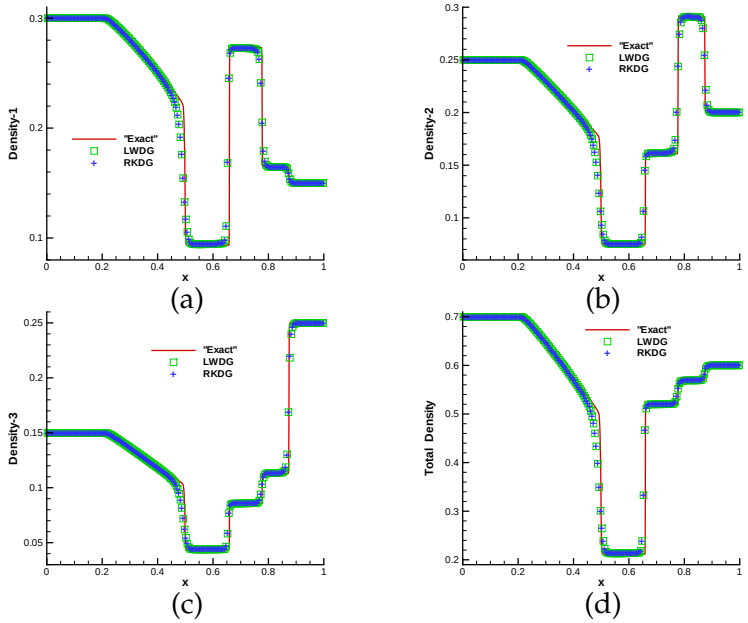

Figure 3: Same as Fig. 1, except for initial condition (c).

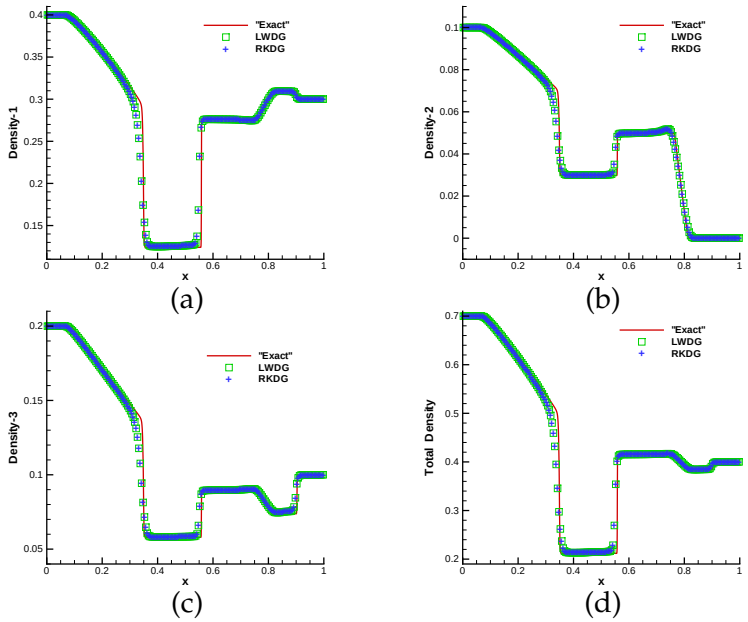

Figure 4: Same as Fig. 1, except for initial condition (d).

that in general the RKDG methods cost about 80 percent more in CPU time than the LWDG methods for this problem, even though the CFL number for the RKDG method used in the computation is 1.5 times of those for LWDG methods because of the limitation on linear stability.

The computed densities ρ_1, ρ_2, ρ_3 by both the LWDG and RKDG methods with k=2 using N=200 cells are plotted at t=0.05 against the reference solution by RKDG methods with k=2 with N=2000 cells in Figs. 1, 2, 3 and 4 for initial condition (a), (b), (c) and (d), respectively.

Table 1: Example 3.1: CPU time. Below IC stands for initial condition.

IC	a	b	c	d
LWDG	10.34375	8.8125	8.53125	8.21875
RKDG	18.65625	15.90625	15.359375	14.8125

We can see that the computed densities ρ_1, ρ_2 and ρ_3 by both the LWDG and RKDG methods have a good agreement to the reference solutions, respectively.

Example 3.2. Traffic signal control problem. Now we apply the developed scheme to the traffic signal control problem, in which the functions of θ are also temporal. This is very common in traffic problems. We use the same data as in [26]. At the stop line which is near x=0.35 on a road with a section length L=1200m, v_f=20m/s and a constant $a(x)$, the signal display turns from green to red(at t=0s) and holds for 30s, and then turns back to green for another 30s. We suppose that all $b_l(x)(l=1,2,3)$ are described by the following:

$$(b_1,b_2,b_3)=\begin{cases}(0,0,0), & \text{if } \ 0.34<x<0.36,\ 0<t-60[t/60]\le 30\text{s},\\ (0.5,0.75,1), & \text{otherwise.}\end{cases}$$

Under these assumptions, the Jacobian matrix $F'(U)$ in Eq. (2.3) is as following:

$$F'(U)=\begin{pmatrix} a_{11} & -\frac{v_f b_1 u_1}{a} & -\frac{v_f b_1 u_1}{a} & a_{14} & 0 & 0\\ -\frac{v_f b_2 u_2}{a} & a_{22} & -\frac{v_f b_2 u_2}{a} & 0 & a_{25} & 0\\ -\frac{v_f b_3 u_3}{a} & -\frac{v_f b_3 u_3}{a} & a_{33} & 0 & 0 & a_{36}\\ 0 & 0 & 0 & 0 & 0 & 0\\ 0 & 0 & 0 & 0 & 0 & 0\\ 0 & 0 & 0 & 0 & 0 & 0 \end{pmatrix},$$

where

$$a_{11}=v_f b_1\Big(1-\frac{u_2+u_3}{a}\Big)-\frac{2v_f b_1 u_1}{a},\quad a_{22}=v_f b_2\Big(1-\frac{u_1+u_3}{a}\Big)-\frac{2v_f b_2 u_2}{a},$$
$$a_{33}=v_f b_3\Big(1-\frac{u_1+u_2}{a}\Big)-\frac{2v_f b_3 u_3}{a},\quad a_{14}=v_f u_1\Big(1-\frac{u_1+u_2+u_3}{a}\Big),$$
$$a_{25}=v_f u_2\Big(1-\frac{u_1+u_2+u_3}{a}\Big),\qquad a_{36}=v_f u_3\Big(1-\frac{u_1+u_2+u_3}{a}\Big).$$

Similar to that in Section 2, we can calculate the derivatives of each component of $F'(U)$ with respect to x and t to get $F'(U)_x$ in Eq.(2.4) and $F'(U)_t$ in Eq.(2.6).

The initial condition of all $\{\rho_l\}_{l=1}^m$ is :

$$\frac{U(x,0)}{a}=(0.05,0.25,0.1)^T, \tag{3.1}$$

and the numerical result is shown in Fig. 5, from which a waiting queue can be clearly seen before the stop line, which propagates backward during the interval before the green signal. Moreover, the total density ρ reaches its maximum in the queue. Fig. 6 demonstrates the whole evolution of the total density in a period of 60s, in which the queuing and dissipation near the

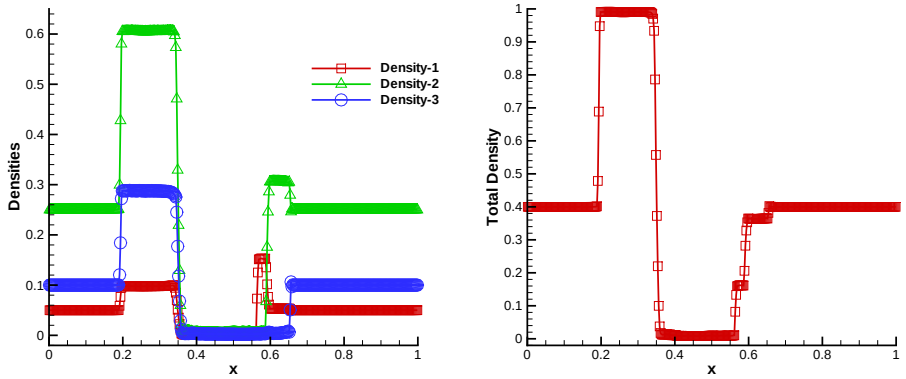

Figure 5: Example 3.2: Densities of all classes at t=30s, k=2 (left); Total density at t=30s, k=2 (right).

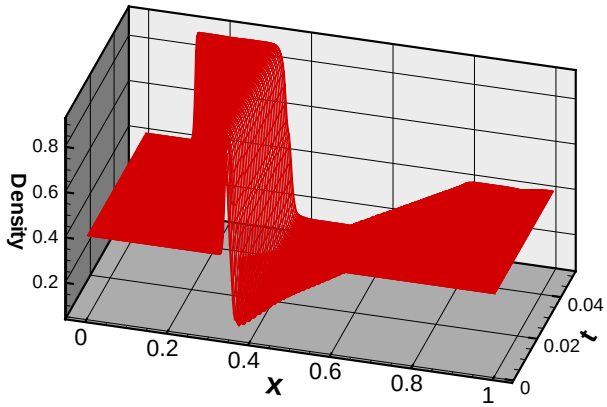

Figure 6: Change of total density for the simulation time T=60s, k=2.

stop line are well reflected. The three shocks appearing on the right-hand side of the stop line represent overtaking between the three types of vehicles.

We can also simulate traffic signal control for any longer time since the change of signal lights is periodic, and set the number of vehicles to be any larger although the code will be quite long and messy.

4 Conclusions

In this paper, the discontinuous Galerkin methods with Lax-Wendroff time discretization is applied to simulate the MCLWR model on an inhomogeneous highway. The numerical examples demonstrate the robustness of the LWDG method using WENO limiters. Since the Lax-Wendroff time discretization is an one step method instead of the multi-step Runge-Kutta time discretization, the LWDG method can save a certain amount of computational cost over the RKDG method; thus is more cost effective. Based on the modified standard hyperbolic conservation system (despite it being non-strictly hyperbolic), the Lax-Friedrichs flux gives correct numerical viscosity for the convergence of the numerical solutions to physically relevant solutions, while the WENO limiting procedure reduces the surplus numerical viscosity to achieve a high level of resolution of the claimed waves.

Acknowledgments

The research was partially supported by NSFC grant 10671091 and JSNSF BK2006511.

References

[1] R. BISWAS, K. D. DEVINE AND J. FLAHERTY, *Parallel, adaptive finite element methods for conservation laws*, Appl. Numer. Math., 14 (1994), pp. 255–283.
[2] B. COCKBURN, S. HOU AND C.-W. SHU, *The Runge-Kutta local projection discontinuous Galerkin finite element method for conservation laws IV: the multidimensional case*, Math. Comput., 54 (1990), pp. 545–581.
[3] B. COCKBURN, S.-Y. LIN AND C.-W. SHU, *TVB Runge-Kutta local projection discontinuous Galerkin finite element method for conservation laws III: one-dimensional systems*, J. Comput. Phys., 84 (1989), pp. 90–113.
[4] B. COCKBURN AND C.-W. SHU, *TVB Runge-Kutta local projection discontinuous Galerkin finite element method for conservation laws II: general framework*, Math. Comput., 52 (1989), pp. 411–435.
[5] B. COCKBURN AND C.-W. SHU, *The Runge-Kutta local projection P1-discontinuous Galerkin finite element method for scalar conservation laws*, Math. Model. Numer. Anal. (M^2AN), 25 (1991), pp. 337–361.
[6] B. COCKBURN AND C.-W. SHU, *The Runge-Kutta discontinuous Galerkin method for conservation laws V: multidimensional systems*, J. Comput. Phys., 141 (1998), pp. 199–224.
[7] C.F. DAGANZO, *A behavioral theory of multi-lane traffic flow, Part I: Long homogeneous freeway sections*, Transportation Research, 36B (2002), pp. 131–158.
[8] C.F. DAGANZO, *A behavioral theory of multi-lane traffic flow, Part II: Merges and the onset of congestion*, Transportation Research 36B (2002), pp. 159–169.
[9] S. GODUNOV, *A difference scheme for numerical computation of discontinuous solution of equations of fluid dynamics*, Mathematics of the USSR-Sbornik, 47 (1959), pp. 271–306.
[10] B. D. GREENSHIELDS, *A study of traffic capacity*, Proceedings of the Highways Research Board, 14 (1934), pp. 448–477.
[11] P.D. LAX AND B. WENDROFF, *Systems of conservation laws*, Commun. Pure Appl. Math., 13 (1960), pp. 217–237.
[12] J. P. LEBACQUE, *The Godunov scheme and waht it means for first order traffic flow model*, in: J.B. Lesort (Ed.), Proceedings of the 13th International Symposium on Transportation and Traffic Theory, Elsevier Science Ltd., Lyon, France, 1996, pp. 647–677.
[13] M.J. LIGHTHILL AND G.B.WHITHAM, *On kinematic waves: II. A theory of traffic flow on long crowded roads*, Proceedings of the Royal Society, London, Series A 229 (1955), pp. 317–345.
[14] J. QIU, M. DUMBSER AND C.-W. SHU, *The discontinuous Galerkin method with Lax-Wendroff type time discretizations*, Comput. Methods Appl. Mech. Engrg., 194 (2005), pp. 4528–4543.
[15] J. QIU AND C.-W. SHU, *Runge-Kutta discontinuous Galerkin method using WENO limiters*, SIAM J. Sci. Comput., 26 (2005), pp. 907–929.
[16] J. QIU AND C.-W. SHU, *Hermite WENO schemes and their application as limiters for Runge-Kutta discontinuous Galerkin method: one dimensional case*, J. Comput. Phys., 193 (2004), pp. 115–135.
[17] P. J. RICHARDS, *Shock waves on the highway*, Operations Research 4 (1956), pp. 42–51.
[18] W.H. REED AND T.R. HILL, Triangular Mesh Methods for Neutron Transport Equation, Tech. Report LA-UR-73-479, Los Alamos Scientific Laboratory, 1973.

[19] C.-W. SHU AND S. OSHER, *Efficient implementation of essentially non-oscillatory shock-capturing schemes*, J. Comput. Phys., 77 (1988), pp. 439–471.
[20] C.-W. SHU, *TVB uniformly high-order schemes for conservation laws*, Math. Comput., 49 (1987), pp. 105–121.
[21] C.-W. SHU, *Essentially non-oscillatory and weighted essentially non-oscillatory schemes for hyperbolic conservation laws*, in: B. Cockburn, C. Johnson, C.-W. Shu, E. Tadmor(Eds.), Advanced Numerical Approximation of Nonlinear Hyperbolic Equations, in: A. Quarteroni (Ed.), Lecture Notes in Mathematics, vol. 1697, Springer, 1988, pp. 325–432.
[22] E. F. TORO AND V. A. TITAREV, *Solution of the generalized Riemann problem for advection-reaction equations*, Proc. Royal Soc. London, 458 (2002), pp. 271–281.
[23] G. C. K. WONG AND S. C. WONG, *A multi-class traffic flow model - an extension of LWR model with heterogeneous drivers*, Transportation Research, 36A (2002), pp. 827–841.
[24] P. ZHANG AND R. X. LIU, *Hyperbolic conservation laws with space-dependent flux: I Characteristics theory and Riemann problem*, J. Comput. Appl. Math., 156 (2003), pp. 1–21.
[25] M. P. ZHANG, C.-W. SHU, G. C. K. WONG AND S. C. WONG, *A weighted essentially non-oscillatory numerical scheme for a multi-class Lighthill-Whitham-Richards traffic flow model*, J. Comput. Phys., 191 (2003), pp. 639–659.
[26] P. ZHANG, S. C. WONG AND C.-W. SHU, *A weighted essentially non-oscillatory numerical scheme for a multi-class traffic flow model on an inhomogeneous highway*, J. Comput. Phys., 212 (2006), pp. 739–756.